International Journal of Nanomedicine

Dovepress
Taylor & Francis Group

Open Access Full Text Article

ORIGINAL RESEARCH

Orally Administrated Inulin-Modified Nanozymes for CT-Guided IBD Theranostics

Xinwen Li[1,*], Lin Cao[1,*], Jianmin Li[2,*], Zhengyang Li[1], Hongyu Ma[3], Shifeng Cheng[1], Hongyi Xu[1], Yang Zhao[1,2]

[1]Department of Radiology, The Second Hospital of Tianjin Medical University, Tianjin, 300211, People's Republic of China; [2]Tianjin Institute of Urology, The Second Hospital of Tianjin Medical University, Tianjin, 300211, People's Republic of China; [3]Image Center, Cangzhou Integrated Traditional and Western Medicine Hospital, Cangzhou, 061000, People's Republic of China

*These authors contributed equally to this work

Correspondence: Yang Zhao, Department of Radiology, The Second Hospital of Tianjin Medical University, Tianjin, 300211, People's Republic of China, Email yang.zhao@tmu.edu.cn

Background: Inflammatory bowel disease (IBD) is a chronic inflammatory bowel disease with no clinical cure. Excessive production of reactive oxygen species (ROS) at the inflammatory sites leads to the onset and progression of IBD. And the current non-invasive imaging methods are not ideal for the diagnosis and monitoring of IBD.

Methods: Herein, we developed inulin (IN)-coated cerium oxide nanoparticles (CeO_2@IN NPs) for treatment and monitoring of IBD guided by computed tomography (CT). The physicochemical properties, ROS scavenging ability and CT imaging capabilities of CeO_2@IN were investigated in vitro. Moreover, the therapeutic and targeted inflammation imaging effects of CeO_2@IN were validated in dextran sulfate sodium (DSS)-induced colitis model.

Results: CeO_2@IN with catalase (CAT) and superoxide dismutase (SOD) capabilities effectively scavenged ROS, thus protecting the cells against oxidative stress. In colitis model mice, orally administered CeO_2@IN successfully traversed the gastrointestinal tract to reach the colon under the protection of IN, and effectively reduced intestinal inflammation, thereby maintaining the intestinal epithelial integrity. Notably, CeO_2@IN performed better than conventional CT contrast agents for gastrointestinal tract imaging, particularly in detecting the inflamed areas in the colon. In addition, CeO_2@IN exhibited excellent biocompatibility in vitro and in vivo.

Conclusion: The study provided a novel integrated diagnostic and therapeutic tool for the treatment and monitoring of IBD, presenting great potential as a clinical application for IBD.

Keywords: inflammatory bowel disease, ceria, nanozyme, antioxidation, CT imaging

Introduction

One of the main characteristics of Inflammatory bowel disease (IBD) is persistent inflammation of the gastrointestinal tract (GIT), and alternating recurrence and remission processes seriously affect patients' daily life and pose a huge economic burden.[1–3] Current therapies for IBD have some drawbacks, such as limited therapeutic effects and adverse side effects.[4–6] Therefore, new strategies are urgently needed for IBD treatment. Abnormal immune activation and excessive reactive oxygen species (ROS) generation are concerned with the onset and advance of IBD.[7,8] During the progression of IBD, toxic ROS induce oxidative stress in colonic mucosal cells, significantly enhancing the intestinal membrane permeability and triggering excessive immune responses, eventually damaging the intestinal mucosa.[9,10] Impaired integrity of the intestinal mucosa enhances the penetration of inflammatory cells and stimulates the synthesis of inflammatory cytokines and ROS. This toxic loop of ROS generation and inflammation contributes to IBD progression.[11] Considering the important role of oxidative stress in IBD pathogenesis, eliminating ROS from inflammatory sites is an extremely effective strategy to treat IBD.[12] Some natural enzymes could reduce the intracellular ROS levels.[12,13] However, the clinical applications of these enzymes are restricted by their low stability, efficiency, potential immunogenicity, and single catalytic activity.[14] With the advent of nanotechnology, nanomedicine has found extensive

Received: 17 October 2024
Accepted: 6 February 2025
Published: 18 February 2025

application in the diagnosis and treatment of cancer.[15–18] Concurrently, nanomedicines exhibiting enzymatic activity demonstrate potential in modulating the redox balance of inflammatory diseases.[19]

Cerium oxide (CeO_2) nanoparticles (NPs) have attracted interest as antioxidant nanozymes served for inflammatory diseases.[20–22] CeO_2 NPs exhibit superoxide dismutase (SOD) and catalase (CAT) activities, thereby removing ROS, including superoxide anions and hydrogen peroxide.[23,24] Additionally, CeO_2 NPs are ideal computed tomography (CT) contrast agents for GIT imaging due to their higher k-edge (40.4 keV) compared to that of iodine (33.2 keV).[24,25] Unlike traditional contrast agents, CeO_2 NPs exhibit enzymatic activities and effectively reduce free radicals generated via X-ray irradiation during imaging, which can minimize the additional damage caused by exogenous stress.[26,27] However, traditional CeO_2-based nanomaterials tend to aggregate and precipitate in aqueous solutions, leading to safety issues and reduced pharmacological efficacy, especially in the complex, acidic, and enzyme-rich gastrointestinal environment.[11,28] Some studies have confirmed that applying a biocompatible coating on the surface of CeO_2 can improve its dispersibility and stability in solution.[22,29,30] Note, these methods either fail to promote collaborative therapeutic effect because of single protective coating[25,31] or may lead to limited clinical translational potential due to the tedious synthetic process.[10]

Inulin (IN) is an inexpensive, safe, and biodegradable natural fructose polymer derived from plants that has been certified as a natural food by the US Food and Drug Administration.[32] IN exhibits resistance to gastric acid and mammalian enzymes and is degraded only by inulinase within the colon, thereby preventing its absorption by the upper GIT.[33–36] Serving as a classic prebiotic, IN metabolized the gut microbiota to promote the proliferation of beneficial gut microbes by maintaining intestinal microecological balance and host health.[37–41] Owing to its beneficial characteristics and selective digestibility in the colon, IN is among the most popular colon-targeting carriers. Moreover, stability, safety, and colon-targeting properties of IN make it a promising agent to overcome the challenges of using CeO_2 NPs in the GIT, facilitating the development of an innovative theranostic strategies to monitor and alleviate intestinal inflammation in IBD.

In this study, we developed and reported that inulin-coated CeO_2 NPs (CeO_2@IN NPs) via a simple one-step alkaline precipitation method, which can be used for CT-guided imaging and IBD treatment. The modification of CeO_2 with IN polysaccharides improves its dispersibility and stability owing to the steric hindrance effect of the polymer.[42] As a natural prebiotic, IN coating on CeO_2 surfaces further protects the NPs from absorption in the upper GIT, conferring targeted specificity for the colon inflammation sites.[43,44] Here, CeO_2@IN NPs exhibit excellent ROS scavenging activity and safeguard the cells from oxidative damage caused by H_2O_2. Furthermore, in vivo studies using a dextran sulfate sodium (DSS)-induced acute colitis mice model revealed that oral administration of CeO_2@IN NPs could accumulate in the inflamed colonic epithelium, downregulate the levels of pro-inflammatory cytokines and significantly reduce body weight loss, colonic injury, and fatality. Notably, CeO_2@IN NPs have shown not only high suitability as CT contrast agents for non-invasive GIT imaging but also excellent biocompatibility both in vitro and in vivo. Therefore, CeO_2@IN NPs exhibit significant potential for the comprehensive diagnosis and therapy of IBD.

Materials and Methods

Materials

Cerium nitrate hexahydrate ($Ce(NO_3)_3{\cdot}6H_2O$), Inulin, sodium hydroxide (NaOH), 2',7'-dichlorodihydrofluorescein diacetate (DCFH-DA), and DSS (MW 40000) were purchased from Aladdin Reagent Co. Ltd. (Shanghai, China). Dihydroethidium (DHE, HY-D0079) was purchased from MCE. Cell Counting Kit (CCK)−8 assay method (Dojindo Laboratory, Japan) was used to detect cell viability. All chemicals were used directly without further purification.

Synthesis of CeO_2@IN

CeO_2@IN was synthesized using a previously described precipitation method.[24] Briefly, IN aqueous solution was made by adding 125 mg IN to 3.5 mL of deionized water. Subsequently, 1 mL $Ce(NO_3)_3{\cdot}6H_2O$ solution (22.5 mg/mL) was added to IN drop-by-drop and stirred for a while at room temperature until well-distributed, and then 80 mM NaOH was added to adjust the pH to 12 and stirred at 37°C for 4 h. As the reaction progresses, the solution turned brown. The suspension was subjected

to centrifugation at 10000 rpm for 10 min in order to eliminate the large aggregates. Finally, the supernatant was washed thrice in ultrafiltration tubes (MWCO 100 kDa) with deionized water at 5000 rpm for 10 min. The ultimate solution was then stored at 4°C until use.

Characterization

Morphology of the precipitated CeO_2@IN was observed using a transmission electron microscope (HT7icr700). Hydrodynamic diameter was determined by the Malvern laser particle size analyzer (Malvern Instruments, UK). UV-vis-NIR spectrophotometer (Hitachi UV-3600 plus, Japan) was used to detect unique peaks of nanoparticles. FT-IR spectra were recorded using the Nicolet iS10 FT-IR spectrometer (Thermo Fisher Scientific, USA). ICP-MS (Spectro Genesis, Germany) was used for quantitative analysis. Confocal microscopy (FV1000; Olympus, Tokyo, Japan) was employed to capture the ROS-sensitive fluorophore images.

Mimetic Enzyme Activity of CeO_2@IN

The SOD-mimicking activity was conducted according to the instructions provided by the total superoxide dismutase assay kit (Beyotime Biotechnology, China). Briefly, 20 μL of CeO_2@IN with different concentration of Ce (25–1000 μg/mL) were introduced into 96-well plates, then followed by the sequential addition of 200 μL of WST-1 working solution and 20 μL of enzyme working solution. After incubation at 37°C for 30 min, the absorbance at 450 nm of mixture was detected by microplate reader.

The CAT-mimicking activity of CeO_2@IN NPs was assessed by analyzing the amount of O_2 generated by the catalytic decomposition of H_2O_2 using a dissolved oxygen electrode. Briefly, H_2O_2 was mixed with different concentrations of CeO_2@IN NPs to maintain a final concentration at 5 mM. The generation of dissolved oxygen was recorded within 600 s for 30 times.

Cell Culture

Human Colon Epithelial-like Carcinoma (HT-29) cell line was obtained by ATCC. HT-29 was cultured in the Roswell Park Memorial Institute-1640 medium (Gibco, China) containing 10% fetal bovine serum and 1% penicillin–streptomycin antibiotics. The cells were cultured in 10-cm cell culture dishes in a 37°C and 5% CO_2 humidified incubator.

Cell Viability Assay

To determine the cytotoxicity of CeO_2@IN NPs, CCK-8 viability assay kit was employed at this section to assess cell viability. First, HT-29 cells were seeded into 96-well plates at a density of 5,000 cells until adhered to the wall. Then, the fresh medium containing different concentrations of CeO_2@IN NPs (0, 5, 10, 25, 50, 100, 200, 400, and 500 μg/mL) was added. After incubated for 24 h at 37°C, the cells were washed thrice with PBS, and incubated with a fresh non-fetal bovine serum medium containing the CCK-8 reagent (10:1) for approximately 2 h at 37°C. Finally, the absorbance at 450 nm of cell was measured by microplate reader.

Detection of ROS

ROS scavenging ability of CeO_2@IN NPs was assayed using DCFH-DA. HT-29 cells were cultured on confocal glass dishes with approximately 5×10^5 cells and left undisturbed for 24 h. Next, a fresh medium containing NPs (200 μg/mL) was changed and cultured for 12 h. Then, the cells, except the control cells, were stimulated with 200 μM H_2O_2 for 6 h. Upon 30 minutes of incubation with DCFH-DA (10 μM), the cells were washed with PBS to eliminate the free dye, and intracellular fluorescence was quantified via confocal laser scanning microscopy.

Establishment of a DSS-Induced Colitis Model and Treatment With CeO_2@IN

Acute ulcerative colitis model was established as previously described.[45] Before the in vivo study, C57BL/6 female mice (6-week-old; 18–20 g) were acclimatized for 1 week and randomly divided into five groups (n = 3/group): healthy control, DSS-induced colitis, 5-ASA-treated colitis, IN-treated colitis, and CeO_2@IN-treated colitis groups. Particularly, DSS-induced colitis models were provided 3% (w/v) DSS aqueous solution for 6 or 7 days, after which DSS was

replaced with pure water. In contrast, healthy control mice only received water. After colitis induction, CeO_2@IN-treated group received an equivalent dosage of Ce (75 mg/kg) via oral gavage every 24 h and underwent CT imaging 12 h following oral administration. In addition, mice in IN-treated group were given 20 mg of inulin[46] orally, and mice in 5-ASA-treated group were given an oral dose of 30 mg/kg[47,48] per day. On day 10, all the mice were sacrificed and the whole colon was gathered for further use. After measuring the length of the colons, one portion of the colonic tissues was preserved for H&E and DHE staining, and another portion was processed into colonic tissue homogenates for the detection of inflammatory factors. All animal experiments complied with the requirements of the Guidelines for the Care and Use of Laboratory Animals of Tianjin University of Traditional Chinese Medicine (China) and received the approval of its Animal Ethics Committee (TCM-LAEC2023041).

CT Scan Procedure

As CeO_2 is the main component of CeO_2@IN NPs that facilitates CT imaging, the Ce content in CeO_2@IN NPs was quantified via ICP-MS. Ioversol, a commercial CT contrast agent, served as the control to study the CT imaging capacity of CeO_2@IN. CT scan images were mainly obtained using a clinical spectral CT scanner (Siemens SOMATOM Definition Edge). First, the CT signals of ioversol and CeO_2@IN solution at the concentrations from 0.5 to 10.0 mg/mL were measured at different tube voltage in vitro. Next, a DSS-induced acute colitis mouse model was established to explore the CT imaging ability of CeO_2@IN NPs in vivo. Three groups including CeO_2@IN-treated healthy mice, CeO_2@IN-treated colitis mice and ioversol-treated colitis mice were gavaged with ioversol or CeO_2@IN NPs at a dose of 75 mg/kg (Ce or I). CT images in vivo were acquired at regular intervals such as 5 min, 30 min, 1 h, 2 h, 4 h, 6 h, 8 h, 10 h, 12 h, and 24 h. The concentration of Ce in colon tissue aggregates was determined using ICP-MS. The accuracy of CT signals was ensured through three different slices from the colon region at 12 h after oral administration with CeO_2@IN.

Biosafety of CeO_2@IN

A daily oral administration of saline or CeO_2@IN NPs was given to healthy female C57BL/6 mice. On day 14, the mice were euthanized, and all major organs and digestive organs were gathered for histological examination. The Ce content of organ samples after 24h oral administration was measured using ICP-MS for analysis. Moreover, blood samples were collected for routine blood tests as well as for assessments of liver and kidney function.

Histological Analysis

After being treated with a 10% paraformaldehyde solution, the obtained tissue samples were embedded in paraffin. Tissue slices of 5 μm in thickness were prepared and then stained using hematoxylin and eosin. Microscopic methods were employed to acquire histological pictures.

Statistical Analyses

Data are represented as the mean ± standard deviation. Analytical procedures were conducted using the GraphPad Prism 9.0 software. The significant differences were tested by the Student's *t*-test for two-group comparisons, one-way ANOVA and two-way ANOVA followed by Tukey's HSD multiple comparison post hoc test. Statistical significance p values were indicated at *P < 0.05, **P < 0.01, ***P < 0.001, and ****P < 0.0001, and ns (not significant).

Results

Synthesis and Characterization of CeO_2@IN

The synthesis of CeO_2@IN NPs was achieved by precipitating cerium salts in the presence of IN, followed by the addition of sodium hydroxide (Figure 1A). Figure 1B showed that the synthetic CeO_2@IN NPs were well suspended in deionized water. The morphology of CeO_2@IN NPs was observed via TEM, revealing a size of around 5 nm (Figure 1C). Using dynamic light scattering, the hydrodynamic diameter of CeO_2@IN NPs was determined to be 8.302 nm (Figure 1D). The UV-visible spectra of CeO_2@IN NPs showed a characteristic absorption peak at 290 nm, which was

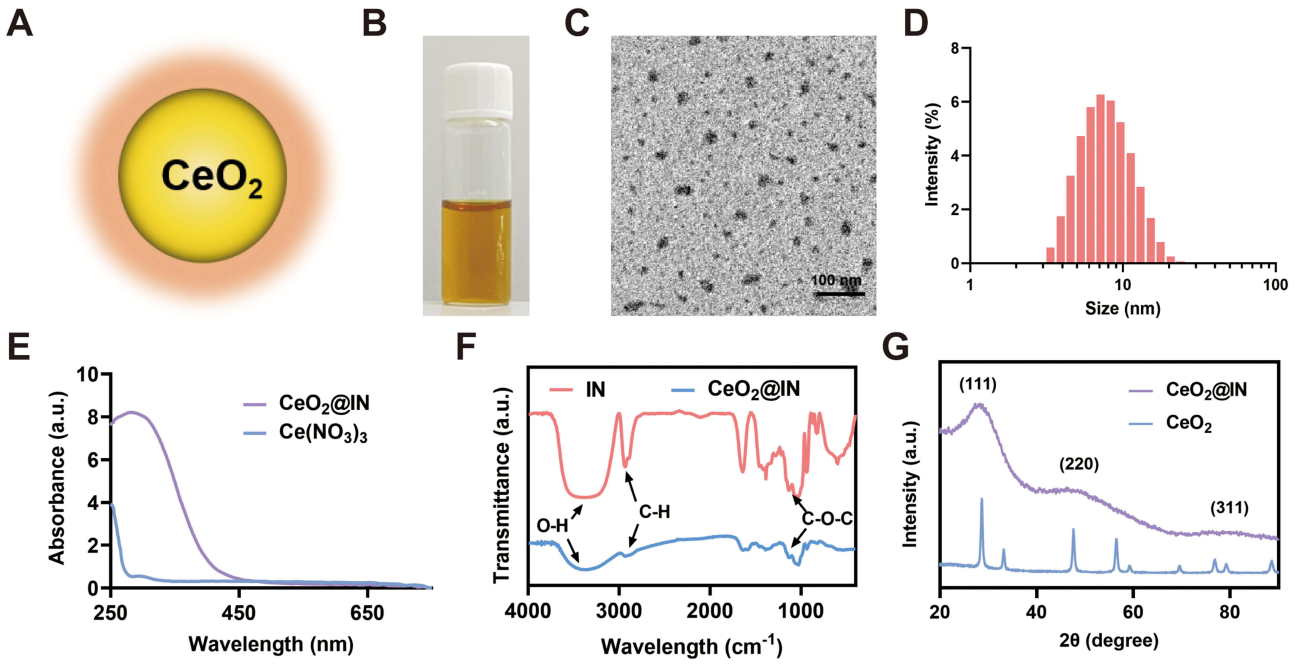

Figure 1 Structural characterization of inulin (IN)-coated cerium oxide nanoparticles (CeO_2@IN NPs). (**A**) Schematic image of CeO_2@IN. (**B**) Photograph of the CeO_2@IN suspension. (**C**) TEM image of CeO_2@IN. (**D**) Particle size analysis of CeO_2@IN via DLS. (**E**) Ultraviolet-visible absorption spectra of CeO_2@IN. (**F**) FT-IR of IN and CeO_2@IN. (**G**) XRD pattern of CeO_2 and CeO_2@IN.

consistent with that of CeO_2 (Figure 1E). FT-IR verified the successful formation of NPs following the surface coating of IN with CeO_2 (Figure 1F). The characteristic peaks of free IN for O−H stretching of hydroxyl group, C−H bond stretching, and C−O−C vibration were observed at approximately 3392, 2924, and 1153 cm^{-1}, respectively, and matched well with those of CeO_2@IN NPs. The crystallographic properties of CeO_2@IN NPs were analysed using X-ray diffraction. Observations in Figure 1G revealed that characteristic peaks of CeO_2 were observed at 2θ = 28.5°, 47.4°, and 76.8°,[49] indicating that IN does not affect the structure of CeO_2. TGA analysis curve of CeO_2@IN NPs within the temperature range the range of 0−850°C in a nitrogen atmosphere revealed that the content of CeO_2 in NPs was approximately 65 wt% (Supplementary Figure 1).

Antioxidant Enzymatic Activities of CeO_2@IN in vitro

Different polymer-modified CeO_2 NPs exhibit enzyme-like activities and are used in various biomedical applications.[50–52] Excessive ROS production is concerned with the onset and advance of IBD.[53–56] Therefore, ROS-eliminating capacity of CeO_2@IN NPs, including their SOD- and CAT-mimetic activities, were investigated in this study. SOD-mimetic catalytic activity was associated with the elimination of $\cdot O_2^-$, which was evaluated by the classic WST-1 method (Figure 2A). CeO_2@IN NPs eliminated $\cdot O_2^-$ in a dose-dependent manner, and the eliminating rate of $\cdot O_2^-$ exceeded 80% at a concentration of 1000 μg/mL. Similarly, CAT-mimetic catalytic activity was investigated by measuring the production of O_2, as it decomposes H_2O_2 generated via $\cdot O_2^-$ disproportionation into H_2O and O_2. As shown in Figure 2B, many bubbles were observed after the interaction between CeO_2@IN NPs and H_2O_2 for 30 min. Besides, CAT-mimicking activity of CeO_2@IN NPs was quantified based on the concentration of dissolved O_2 formed via H_2O_2 decomposition in a time-dependent manner (Figure 2C). Moreover, an in vitro inflammatory model was established by stimulating cells with H_2O_2 to assess whether CeO_2@IN NPs protect the cells from ROS-induced damage. In the presence of H_2O_2, intracellular ROS levels were elevated, with green fluorescence emitted from ROS-sensitive probe. However, CeO_2@IN NPs significantly reduced the intracellular ROS levels in H_2O_2-treated cells (Figure 2D). These results suggest that CeO_2@IN NPs exhibit excellent nanozymes activities, showing significant potential for antioxidant IBD treatment.

https://doi.org/10.2147/IJN.S497558

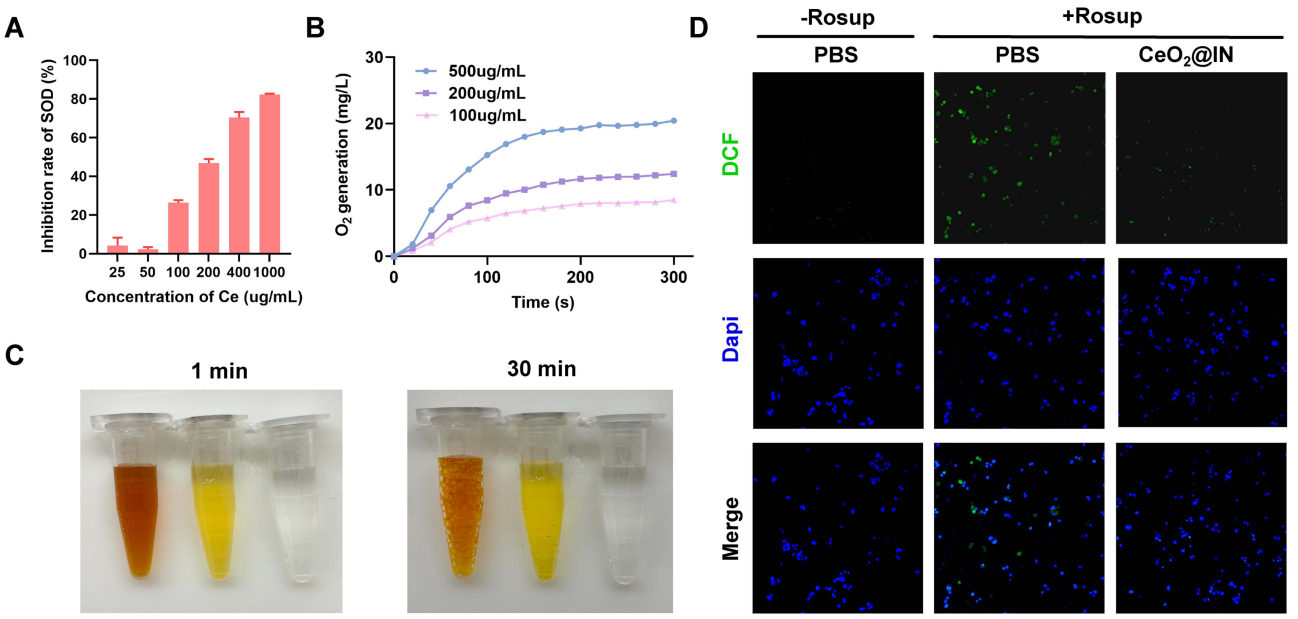

Figure 2 Antioxidant enzymatic activities of CeO_2@IN NPs in vitro. (**A**) SOD- mimicking activity of CeO_2@IN. (**B**) Oxygen generation from H_2O_2 (5 mM) catalyzed by the CAT-mimicking activity of CeO_2@IN. (**C**) Oxygen production via catalysis of H_2O_2 with different concentrations of CeO_2@IN (left: 1000 μg/mL; middle: 100 μg/mL; right: water). (**D**) ROS scavenging activity in H_2O_2-stimulated HT-29 cells determined by evaluating the fluorescence of 2',7'-dichlorodihydrofluorescein diacetate (DCFH-DA).

CT Imaging Potential of CeO_2@IN

To evaluate the CT imaging properties of CeO_2@IN NPs, ioversol, a commercial CT contrast agent, was used as a control. As shown in Figure 3A, CT signals of CeO_2@IN NPs significantly increased with increasing concentration at different voltages. Statistical analysis revealed a linear correlation between the CT signals and Ce concentration at each tube voltage (Figure 3B). CT values of CeO_2@IN NPs were higher than those of ioversol at the same concentration (Figure 3C–D). This was due to the slightly higher K-edge value of Ce (40.4 keV) compared to that of iodine (33.2 keV), which fits better with the X-ray beam energy in clinical practice.[57] These results highlight the excellent CT imaging performance of CeO_2@IN NPs.

Next, we investigated the feasibility of using CeO_2@IN NPs as CT contrast agent for non-invasive and real-time GIT imaging in a DSS-induced colitis mice model. Colitis and healthy mice were orally administered CeO_2@IN NPs or ioversol. CT scans were recorded at scheduled time intervals. After oral administration of CeO_2@IN NPs for 5 min in healthy mice (Figure 3E), GIT imaging was performed for approximately 6 h, proving that CeO_2@IN NPs exhibited excellent imaging capacity in vivo. Notably, GIT of colitis mice treated with CeO_2@IN NPs gradually became visible at 30 min after oral administration, and the remarkable CT contrast enhancement was retained in the large intestine for 12 h (Figure 3E). In contrast, ioversol was enriched in the GIT at 30 min after administration and was almost completely metabolized from the GIT at 6 h in colitis mice. As shown in Figure 3F, a high CT signal at 12 h was only shown in the colonic region of group treated with CeO_2@IN NPs and DSS, which indicated that CeO_2@IN NPs not only effectively detected inflammation compare with healthy mice but also possessed higher sensitivity in inflammatory sites than conventional contrast agents. H&E staining also confirmed the presence of inflammation in these colonic regions (Supplementary Figure 2). Quantitative analysis of Ce via ICP-MS revealed the accumulation of NPs in the inflammatory region (Figure 3G). Accumulation at the inflammatory sites for up to 12 h confirmed the potential of CeO_2@IN NPs for real-time colitis-targeted imaging in vivo.

In vivo Therapeutic Efficacy of CeO_2@IN Treatment

After determining their antioxidant effects in vitro, therapeutic effects of CeO_2@IN NPs were investigated in DSS-induced colitis mice, which are commonly used animal models for the study of human ulcerative colitis.[58] IBD mice

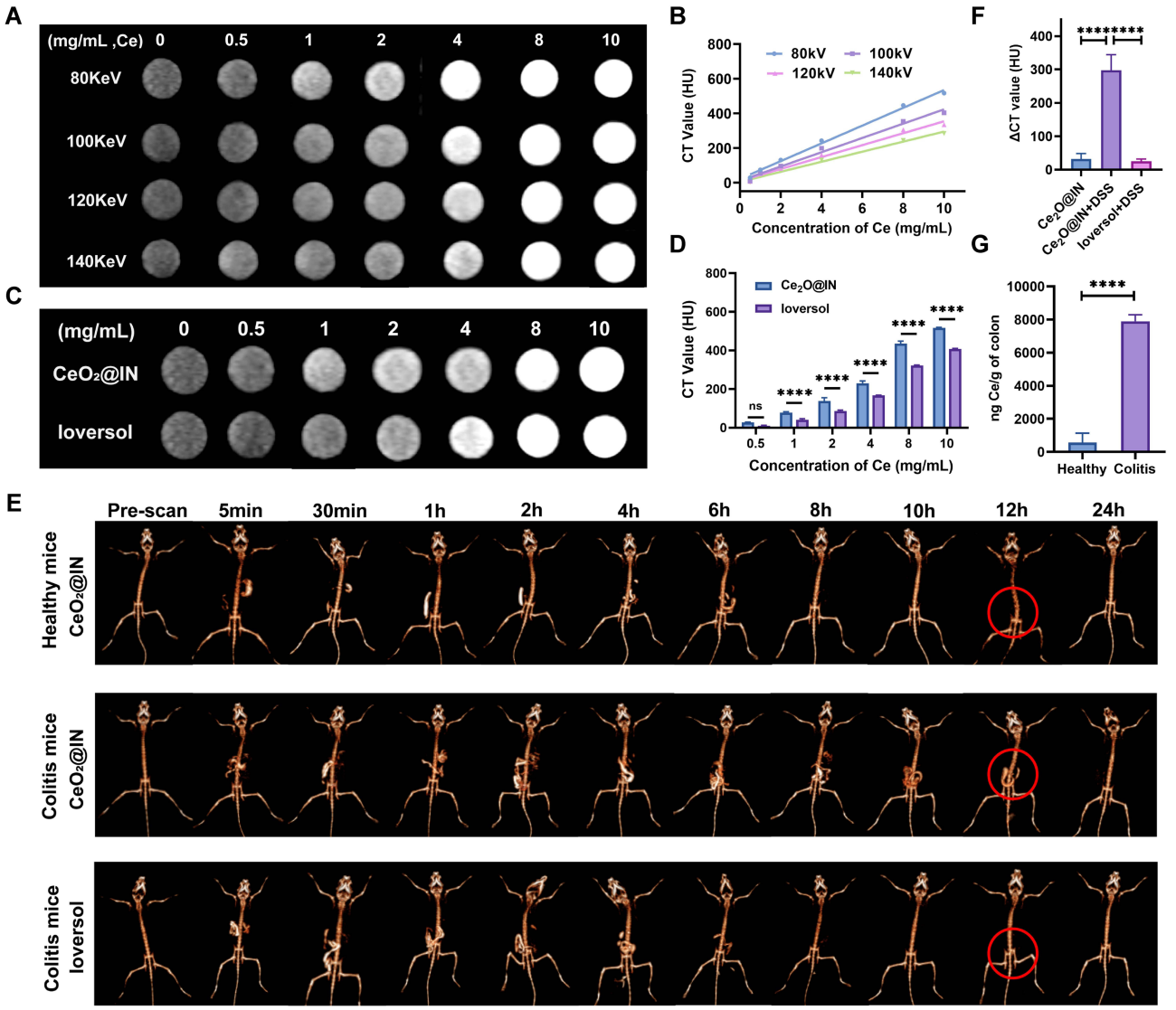

Figure 3 CT imaging potential of CeO_2@IN NPs. In vitro CT scans (**A**) and the linear correlations (**B**) between the CT values and CeO_2@IN concentrations at different voltages. In vitro CT imaging (**C**) and corresponding CT values (**D**) of CeO_2@IN or ioversol at different concentrations at 80 KeV. (**E**) Gastrointestinal tract imaging following oral treatment of CeO_2@IN or ioversol in DSS-induced colitis and healthy mice. **(F)** CT signal quantification of the large intestine of healthy mice treated with CeO_2@IN, colitis mice treated with CeO_2@IN and colitis mice treated with ioversol after oral administration for 12 h. (**G**) Relative Ce contents in the colonic tissues of healthy and colitis groups 12 h following oral CeO_2@IN delivery. The data are presented as the mean ± SD (n=3). ****P < 0.0001. These results were analyzed by *T*-test, one-way and two-way ANOVA followed by Tukey's HSD multiple comparison post hoc test.

models were established by continuous administration of 3% (w/v) dextran sodium sulfate (DSS) for 7 days and given different treatments. Subsequently, we directly adopted 5-aminosalicylic acid (5-ASA),[59,60] a clinically available first-line agent, as a control group for comparison of the therapeutic effects of drugs and CeO_2@IN NPs in order to enrich our research.

As shown in Figure 4A-B, CeO_2@IN NPs protected the mice from DSS-induced shortening of colon length, a characteristic feature of colitis.[61] Similarly, spleen index (the percentage of spleen-to-body weight) of CeO_2@IN NPs group was significantly lower compared with the groups treated by 5-ASA or IN (Figure 4C). To overall assess the therapeutic efficacy of CeO_2@IN NPs, MPO and classical pro-inflammatory cytokine levels were evaluated. MPO activity in colon tissues is directly correlated to the severity of neutrophil infiltration and serves an oxidative stress marker.[62,63] MPO activity was significantly elevated in the colitis group, but such effect was reversed by CeO_2@IN NPs (Figure 4D). Additionally, levels of classic pro-inflammatory cytokines in colon tissues, such as IL-6, and TNF-α, were also increased in the colitis group but normalized by CeO_2@IN NPs treatment (Figure 4E–F). In contrast, there was no

https://doi.org/10.2147/IJN.S497558

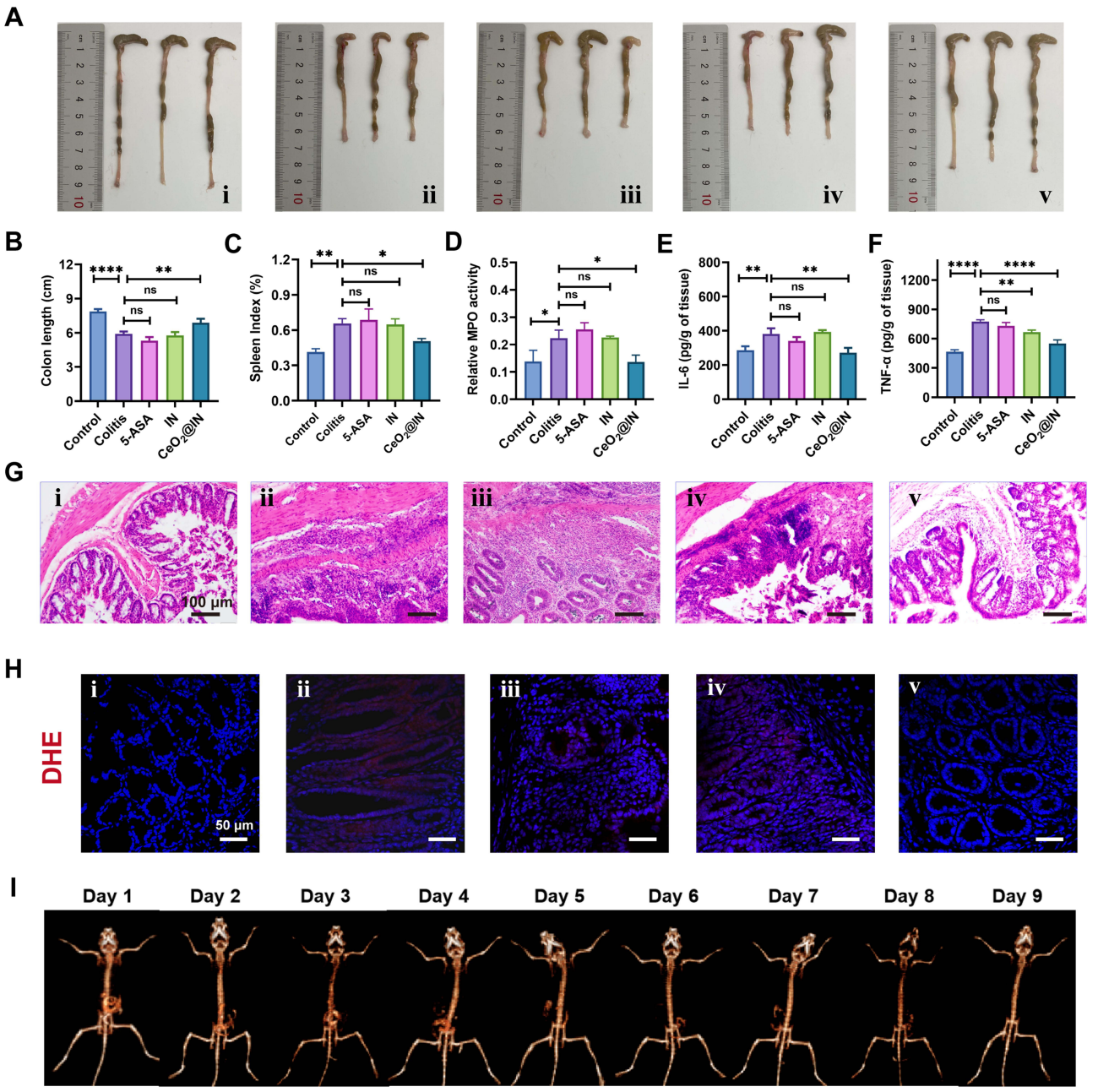

Figure 4 Therapeutic efficacy of CeO_2@IN NPs in DSS-induced colitis mice. Photograph of the representative colon tissues (**A**) and lengths (**B**) removed from healthy and colitis mice 10 d after various treatments (i, control; ii, colitis; iii, 5-ASA; iv, IN; v, CeO_2@IN). (**C**) Spleen index from mice in different groups. Levels of MPO (**D**), IL-6 (**E**), and TNF-α (**F**) in the colonic tissues of all groups 10-d after different treatments. (**G**) H&E staining images of colonic tissues. Scales bars, 100 μm. (**H**) ROS fluorescent imaging of colon tissues stained by DHE in different groups. Scales bars, 50 μm. (**I**) Representative CT images of mice 12 h following oral CeO_2@IN treatment. Data are represented as the mean ± SD (n=3). One-way ANOVA followed by Tukey's HSD multiple comparison post hoc test was performed for statistical analysis. *P<0.05, **P<0.01, ****P<0.0001, ns (not significant).

statistically significant difference in MPO and IL-6 levels between the colitis and 5-ASA or IN groups. And IN-treated group only slightly reduced the content of TNF-α. These findings suggested that CeO_2@IN NPs effectively alleviated DSS-induced colitis symptom.

Moreover, H&E staining was performed to evaluate the pathological damage of colon tissue to prove the therapeutic effect of CeO_2@IN NPs in vivo. In the colitis group, H&E staining of colon tissue revealed severe histological damage, including high inflammatory cell infiltration, crypt disappearance and decreased proportions of goblet cell. However, treatment with CeO_2@IN NPs significantly alleviated this pathological damage. In contrast, partial recovery of colon

shortening and colonic tissue damage were observed in IN-treated colitis mice group, possibly due to the prebiotic property of IN.[46] And the degree of colonic histological damage in the 5-ASA-treated colitis mice group demonstrated the same trend as that in the IN-treated group (Figure 4G). Subsequently, we assessed the presence of $\cdot O_2^-$ in the colonic area of mice by DHE fluorescence staining (Figure 4H). The control and CeO_2@IN NPs groups displayed minimal red fluorescence, but the other group, including DSS group, 5-ASA group and IN group, existed notable red fluorescence. These results highlight the ROS-eliminating capacity of CeO_2@IN NPs in vivo.

In addition to their potent anti-inflammatory effects, CeO_2@IN NPs showed excellent capacity for CT imaging. We further assessed the potential of CeO_2@IN for CT imaging-based therapy of IBD. The 3D-reconstruction CT images of changes at the GIT inflammation site during treatment are shown in Figure 4I and Supplementary Figure 3. At the beginning of treatment, the large intestine of mice with colitis exhibited pronounced CT signals. As the treatment progressed, CT signals in the abdomen of mice narrowed, and no significant CT signals were detected in the same region of the mice after nine days. This decrease in CT signals within the large intestine was attributed to the accelerated metabolism of CeO_2@IN NPs, which decreased the intestinal inflammation and restored the inflammation-related indicators. Taken together, these findings suggest that CeO_2@IN NPs exert potent anti-inflammatory effects and facilitate the real-time non-invasive monitoring of treatment response in IBD.

Biocompatibility of CeO_2@IN

Good biocompatibility is essential as it directly affects the clinical application of nanomedicines. Therefore, potential toxicity of CeO_2@IN NPs was systematically evaluated in this study. First, cytotoxicity was evaluated in HT-29 cells using the cell counting kit (CCK)-8 assay. Even at high concentrations of 500 μg/mL for 24 h, the viability of HT-29 cells exposed to CeO_2@IN remained in excess of 90% (Figure 5A). Oral administration of CeO_2@IN was studied in healthy C57BL/6 mice for either 1 or 14 days. Vital organs and blood were extracted for further detection and histological analyses. As displayed in Figure 5B and Supplementary Figure 4, no obvious histological changes were observed in the H&E-stained images of the digestive and other major organs (heart, liver, spleen, lungs, and kidneys) in the control and 1- or 14-d treatment groups. Similarly, the blood routine and biochemical indicators for both the control group and the groups CeO_2@IN NPs treated for 1- or 14-days were within the normal range (Figure 5C-D).

Then, metabolic clearance of CeO_2@IN NPs in vivo was evaluated by detecting the Ce levels in the vital organs and feces of healthy mice 24 h after post-administration of CeO_2@IN NPs, and PBS was used as the control. ICP-MS analysis showed that the Ce content in major organs was at a low level after oral administration of CeO_2@IN NPs in mice at 24 h, which was the same as that in the control group (Supplementary Figure 5A). However, the content of Ce in feces accounted for 62% of the total intake, which was significantly higher than that in the control group (Supplementary Figure 5B). According to the above results, CeO_2@IN NPs were almost entirely excreted from the body through the gastrointestinal tract within 24 hours. These results indicated that CeO_2@IN NPs did not exert significant adverse effects, suggesting their potential for clinical application.

Discussion

IBD is a chronic inflammatory bowel disease, with limited therapeutic effects of conventional treatment and severe systemic side effects.[4] Excessive production of reactive oxygen species (ROS) at the inflammatory sites leads to the onset and progression of IBD.[64] And the current non-invasive imaging methods are not ideal for the diagnosis and monitoring of IBD. There is a need to develop novel theranostics strategy. In this study, we synthesized inulin (IN)-coated cerium oxide nanoparticles (CeO_2@IN NPs), which possess excellent antioxidant properties and CT imaging capabilities, enabling effective treatment and real-time monitoring of DSS-induced colitis in mice.

Recently, nanozymes with potent antioxidant effects have attracted considerable attention and have been widely used in the treatment for inflammatory diseases, such as cerium oxide (CeO_2) nanoparticles.[65,66] The coexistence and interconversion of Ce^{3+} and Ce^{4+} sites on the surface of CeO_2 nanoparticles engenders nanozymes activity, enabling them to catalyze the removal of various ROS.[67] It is well known that CeO_2 NPs tend to aggregate and precipitate in aqueous solutions, which greatly reduces their scope of application.[68] A biocompatible coating can improve the stability of CeO_2 NPs and retain catalytic capacity. Inulin (IN) exhibits acid resistance and possesses prebiotic properties, making

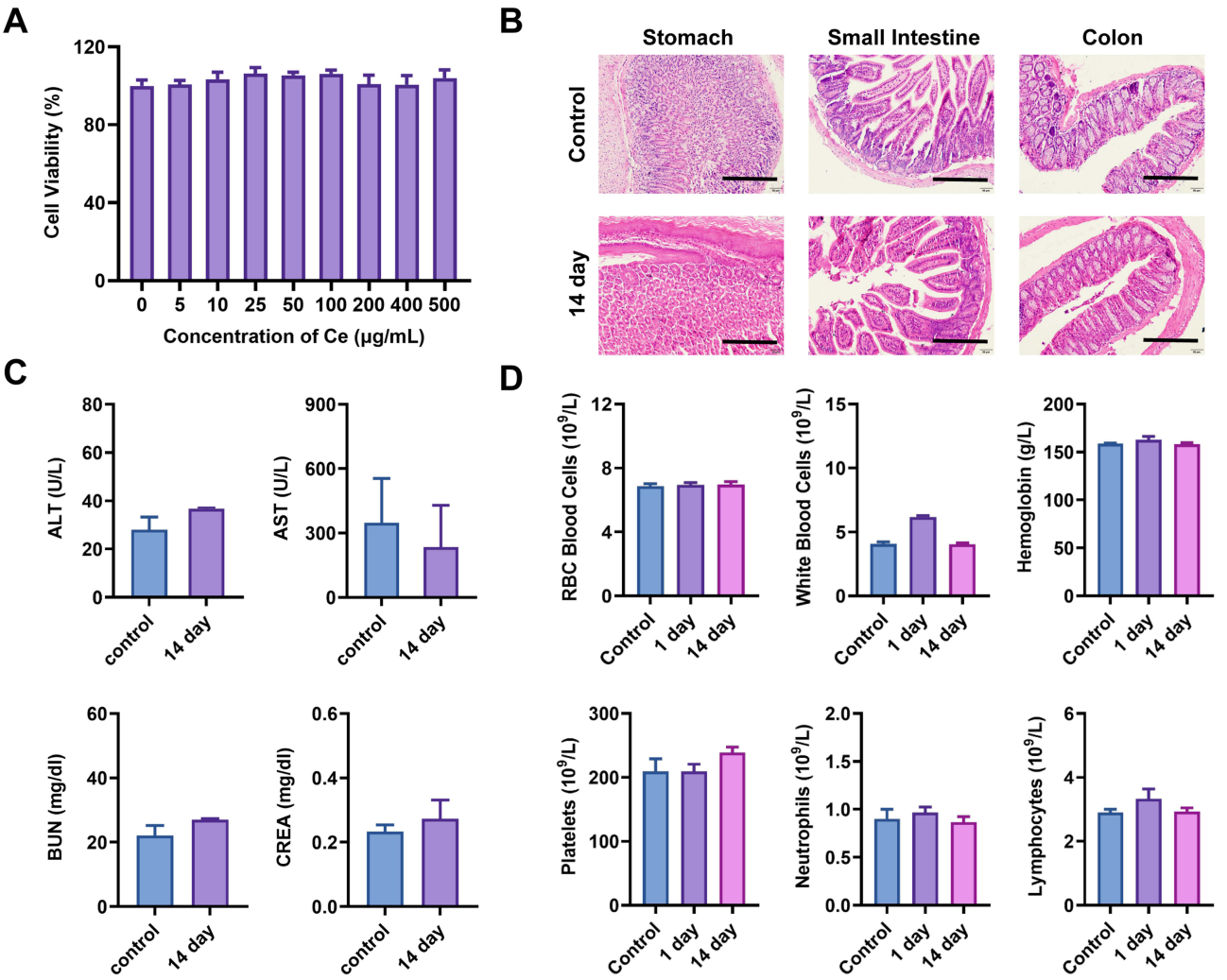

Figure 5 Biocompatibility of CeO_2@IN NPs. (**A**) Cell viability of CeO_2@IN. Blood indices (**B**), liver/kidney functions (**C**), and H&E staining of the digestive organs (**D**) in C57BL/6 mice 1- or 14-d post-administration of CeO_2@IN. Scales bars, 200 μm.

it a commonly utilized carrier for gastrointestinal pharmaceuticals.[69–71] For example, one of the main constituents of salazosulfapyridine (SASP), a clinical first-line agent for IBD, is IN.[72] In addition, IN, as a natural fructose polymer, contributes to increase the bio-adhesion and prolong colon retention, thereby enhancing the drug concentration in the colon.[73,74] Inspired by these studies, we adopted a simple method to modify the IN on the surface of CeO_2 NPs to overcome the above shortcomings. The results showed that the CeO_2@IN NPs demonstrated excellent SOD and CAT mimicking enzyme capabilities as well as good biosafety. Furthermore, CeO_2@IN NPs performed better than conventional CT contrast agents in gastrointestinal imaging due to the high K-edge value of Ce (40.4 keV) compared to that of iodine (33.2 keV), which represented an additional factor contributing to clinical conversion.

To further explore the clinical potential of CeO_2@IN NPs, therapeutic effects of CeO_2@IN NPs were investigated in DSS-induced colitis mice. CeO_2@IN NPs treatment was confirmed to result in significant remission of colonic lesions in mice, including lower spleen index, milder colon shortening, milder pathological changes, and marked reduction of pro-inflammatory factors. Continuous CT imaging monitoring also showed improvement in the colonic lesions, which was consistent with the above biomarkers. The superior therapeutic and imaging outcomes indicated that CeO_2@IN NPs hold significant potential as a novel theranostic agent for CT-guided IBD treatment.

There are also some limitations in our study. We only used the DSS-induced colitis model to verify the effect of CeO_2@IN NPs in alleviating colonic inflammation. However, the therapeutic effect of CeO_2@IN NPs on intestinal injury induced by other chemicals, such as TNBS, has not been investigated. Besides, recurrent inflammation often leads to the

occurrence of chronic colitis, and more seriously, colitis-related colon cancer (CRC) and other complications. Whether the CeO_2@IN NPs treatment can prevent progressive disease and occurrence of complications remains unclear.

Conclusion

In conclusion, our study focused on developing an effective strategy for IBD diagnosis and therapy. We successfully designed and constructed inulin-modified nanozymes, CeO_2@IN NPs. CeO_2@IN NPs exhibited excellent gastrointestinal stability and colitis-targeting, ROS scavenging, and CT imaging capacities. In vivo and in vitro studies revealed that CeO_2@IN NPs exhibited potent SOD- and CAT-mimetic enzyme activities and accumulated in the colitis tissues. In DSS-induced colitis mice, CeO_2@IN NPs not only alleviated inflammation by reducing inflammatory cell infiltration and pro-cytokine production but also facilitated real-time monitoring of treatment efficacy via CT imaging. Furthermore, the developed CeO_2@IN NPs were easily excreted and cleared from the body, exhibited good biosafety and simple synthesis process, suggesting their potential for clinical translation. In summary, our findings suggest CeO_2@IN NPs hold significant potential as promising novel theranostic agents for CT-guided IBD therapy.

Acknowledgments

The authors want to appreciate Animal Ethics Committee of Tianjin University of Traditional Chinese Medicine (China) for professional animal ethics review to ensure compliance in animal experiment segments.

Funding

This research was funded by the Scientific and Technological Research Program of Tianjin Municipal Education Commission (No. 2019ZD025).

Disclosure

The author(s) report no conflicts of interest in this work.

References

1. Olovo CV, Ocansey DKW, Ji Y, Huang XX, Xu M. Bacterial membrane vesicles in the pathogenesis and treatment of inflammatory bowel disease. *Review Gut Microbes*. 2024;16(1):32.2341670. doi:10.1080/19490976.2024.2341670
2. Zhao M, Gonczi L, Lakatos PL, Burisch J. The burden of inflammatory bowel disease in Europe in 2020. *J Crohn's Colitis*. 2021;15(9):1573–1587. doi:10.1093/ecco-jcc/jjab029
3. Park KT, Ehrlich OG, Allen JI, et al. The cost of inflammatory bowel disease: an initiative from the crohn's & colitis foundation. *Inflamm Bowel Dis*. 2020;26(1):1–10. doi:10.1093/ibd/izz104
4. Papamichael K, Afif W, Drobne D, et al. Therapeutic drug monitoring of biologics in inflammatory bowel disease: unmet needs and future perspectives. *Review Lancet Gastroenterol Hepatol*. 2022;7(2):171–185. doi:10.1016/S2468-1253(21)00223-5
5. Shen B, Kochhar GS, Rubin DT, et al. Treatment of pouchitis, Crohn's disease, cuffitis, and other inflammatory disorders of the pouch: consensus guidelines from the international ileal pouch consortium. *Lancet Gastroenterol Hepatol*. 2022;7(1):69–95. doi:10.1016/s2468-1253(21)00214-4
6. Nielsen OH, Gubatan JM, Juhl CB, Streett SE, Maxwell C. Biologics for inflammatory bowel disease and their safety pregnancy: a systematic review and meta-analysis. *Review Clin Gastroenterol Hepatol*. 2022;20(1):74. doi:10.1016/j.cgh.2020.09.021
7. Khor B, Gardet A, Xavier RJ. Genetics and pathogenesis of inflammatory bowel disease. *Nature*. 2011;474(7351):7351):307–317. doi:10.1038/nature10209
8. Zhu H, Li YR. Oxidative stress and redox signaling mechanisms of inflammatory bowel disease: updated experimental and clinical evidence. *Review Exp Biol Med*. 2012;237(5):474–480. doi:10.1258/ebm.2011.011358
9. Huang LJ, Mao XT, Li YY, et al. Multiomics analyses reveal a critical role of selenium in controlling T cell differentiation in Crohn's disease. *Immunity*. 2021;54(8):1728–1744e7. doi:10.1016/j.immuni.2021.07.004
10. Min DK, Kim YE, Kim MK, Choi SW, Park N, Kim J. Orally administrated inflamed colon-targeted nanotherapeutics for inflammatory bowel disease treatment by oxidative stress level modulation in colitis. *ACS Nano*. 2023;17(23):24404–24416. doi:10.1021/acsnano.3c11089
11. Hou L, Gong F, Liu B, et al. Orally administered titanium carbide nanosheets as anti-inflammatory therapy for colitis. *Theranostics*. 2022;12(8):3834–3846. doi:10.7150/thno.70668
12. Zhang B, Li Q, Xu Q, Li B, Dong H, Mou Y. Polydopamine modified ceria nanorods alleviate inflammation in colitis by scavenging ROS and regulating macrophage M2 polarization. *Int J Nanomed*. 2023;18:4601–4616. doi:10.2147/IJN.S416049
13. Zhao H, Zhang R, Yan X, Fan K. Superoxide dismutase nanozymes: an emerging star for anti-oxidation. *J Mater Chem B*. 2021;9(35):6939–6957. doi:10.1039/d1tb00720c
14. Datta S, Rajnish KN, George Priya Doss C, Melvin Samuel S, Selvarajan E, Zayed H. Enzyme therapy: a forerunner in catalyzing a healthy society? *Expert Opin Biol Ther*. 2020;20(10):1151–1174. doi:10.1080/14712598.2020.1787980
15. Tan T, Feng Y, Wang W, et al. Cabazitaxel-loaded human serum albumin nanoparticles combined with TGFβ-1 siRNA lipid nanoparticles for the treatment of paclitaxel-resistant non-small cell lung cancer. *Cancer Nanotechnol*. 2023;14(1). doi:10.1186/s12645-023-00194-7

16. Nie Y, Li D, Peng Y, et al. Metal organic framework coated MnO_2 nanosheets delivering doxorubicin and self-activated DNAzyme for chemo-gene combinatorial treatment of cancer. *Int J Pharm*. 2020:585. doi:10.1016/j.ijpharm.2020.119513.
17. He X, Jiang Z, Akakuru OU, Li J, Wu A. Nanoscale covalent organic frameworks: from controlled synthesis to cancer therapy. *Chem Commun*. 2021;57(93):12417–12435. doi:10.1039/d1cc04846e
18. Wang Y, Xu Y, Song J, et al. Tumor cell-targeting and tumor microenvironment–responsive nanoplatforms for the multimodal imaging-guided photodynamic/photothermal/chemodynamic treatment of cervical cancer. *Int J Nanomed*. 2024;19:5837–5858. doi:10.2147/ijn.S466042
19. Wang H, Li B, Sun Y, et al. NIR-II AIE luminogen-based erythrocyte-like nanoparticles with granuloma-targeting and self-oxygenation characteristics for combined phototherapy of tuberculosis. *Adv Mater*. 2024;36(38). doi:10.1002/adma.202406143
20. Yin Y, Yang J, Pan Y, et al. Mesopore to macropore transformation of metal–organic framework for drug delivery in inflammatory bowel disease. *Adv Healthcare Mater*. 2021;10(3):2000973. doi:10.1002/adhm.202000973
21. Deng J, Yu B, Chang Z, et al. Cerium oxide-based nanozyme suppresses kidney calcium oxalate crystal depositions via reversing hyperoxaluria-induced oxidative stress damage. *J Nanobiotechnol*. 2022;20(1):516. doi:10.1186/s12951-022-01726-w
22. Cao L, Duan D, Peng J, et al. Oral enzyme-responsive nanoprobes for targeted theranostics of inflammatory bowel disease. *J Nanobiotechnol*. 2024;22(1):484. doi:10.1186/s12951-024-02749-1
23. Zeng Z, He X, Li C, et al. Oral delivery of antioxidant enzymes for effective treatment of inflammatory disease. *Biomaterials*. 2021;271:120753. doi:10.1016/j.biomaterials.2021.120753
24. Naha PC, Hsu JC, Kim J, et al. Dextran-coated cerium oxide nanoparticles: a computed tomography contrast agent for imaging the gastrointestinal tract and inflammatory bowel disease. *Article ACS Nano*. 2020;14(8):10187–10197. doi:10.1021/acsnano.0c03457
25. Cao Y, Cheng K, Yang M, et al. Orally administration of cerium oxide nanozyme for computed tomography imaging and anti-inflammatory/anti-fibrotic therapy of inflammatory bowel disease. *J Nanobiotechnol*. 2023;21(1):21. doi:10.1186/s12951-023-01770-0
26. Nie J, Peng C, Pei W, et al. A novel role of long non-coding RNAs in response to X-ray irradiation. *Toxicol In Vitro*. 2015;30(1 Pt B):536–544. doi:10.1016/j.tiv.2015.09.007
27. Cervelli T, Panetta D, Navarra T, et al. A new natural antioxidant mixture protects against oxidative and DNA damage in endothelial cell exposed to low-dose irradiation. *Oxid Med Cell Longev*. 2017;2017(1):9085947. doi:10.1155/2017/9085947
28. Zhang Q, Tao H, Lin Y, et al. A superoxide dismutase/catalase mimetic nanomedicine for targeted therapy of inflammatory bowel disease. *Biomaterials*. 2016;105:206–221. doi:10.1016/j.biomaterials.2016.08.010
29. Shcherbakov AB, Reukov VV, Yakimansky AV, et al. CeO_2 nanoparticle-containing polymers for biomedical applications: a review. *Polymers*. 2021 ;13(6):924. doi:10.3390/polym13060924
30. Zeng M, Zhang X, Tang J, et al. Conservation of the enzyme-like activity and biocompatibility of CeO_2 nanozymes in simulated body fluids. 10.1039/D3NR03524G. *Nanoscale*. 2023;15(35):14365–14379. doi:10.1039/D3NR03524G
31. Huang Y, Xu J, Sun G, et al. Enteric-coated cerium dioxide nanoparticles for effective inflammatory bowel disease treatment by regulating the redox balance and gut microbiome. *Biomaterials*. 2025;314:122822. doi:10.1016/j.biomaterials.2024.122822
32. Shoaib M, Shehzad A, Omar M, et al. Inulin: properties, health benefits and food applications. *Review Carbohydr Polym*. 2016;147:444–454. doi:10.1016/j.carbpol.2016.04.020
33. Mensink MA, Frijlink HW, Maarschalk KV, Hinrichs WLJ. Inulin, a flexible oligosaccharide. II: review of its pharmaceutical applications. *Review Carbohydr Polym*. 2015;134:418–428. doi:10.1016/j.carbpol.2015.08.022
34. Chambers ES, Viardot A, Psichas A, et al. Effects of targeted delivery of propionate to the human colon on appetite regulation, body weight maintenance and adiposity in overweight adults. *Gut*. 2015;64(11):1744–1754. doi:10.1136/gutjnl-2014-307913
35. Walz M, Hagemann D, Trentzsch M, Weber A, Henle T. Degradation studies of modified inulin as potential encapsulation material for colon targeting and release of mesalamine. *Article Carbohydr Polym*. 2018;199:102–108. doi:10.1016/j.carbpol.2018.07.015
36. Giri S, Dutta P, Giri TK. Inulin-based carriers for colon drug targeting. *J Drug Deliv Sci Technol*. 2021;64:14.102595. doi:10.1016/j.jddst.2021.102595
37. Tremaroli V, Bäckhed F. Functional interactions between the gut microbiota and host metabolism. *Nature*. 2012;489(7415):7415):242–249. doi:10.1038/nature11552
38. Vandeputte D, Falony G, Vieira-Silva S, et al. Prebiotic inulin-type fructans induce specific changes in the human gut microbiota. *Gut*. 2017;66(11):1968–1974. doi:10.1136/gutjnl-2016-313271
39. Li K, Zhang L, Xue J, et al. Dietary inulin alleviates diverse stages of type 2 diabetes mellitus *via* anti-inflammation and modulating gut microbiota in db/db mice. *Article Food Funct*. 2019;10(4):1915–1927. doi:10.1039/c8fo02265h
40. Chambers ES, Byrne CS, Morrison DJ, et al. Dietary supplementation with inulin-propionate ester or inulin improves insulin sensitivity in adults with overweight and obesity with distinct effects on the gut microbiota, plasma metabolome and systemic inflammatory responses: a randomised crossover trial. *Gut*. 2019;68(8):1430–1438. doi:10.1136/gutjnl-2019-318424
41. Han K, Nam J, Xu J, et al. Generation of systemic antitumour immunity via the in situ modulation of the gut microbiome by an orally administered inulin gel. *Nat Biomed Eng*. 2021;5(11):15. doi:10.1038/s41551-021-00749-2
42. Wang M, He H, Liu D, Ma M, Preparation ZY. Characterization and multiple biological properties of peptide-modified cerium oxide nanoparticles. *Biomolecules*. 2022;12(9):1277. doi:10.3390/biom12091277
43. Hou Y, Jin J, Duan H, et al. Targeted therapeutic effects of oral inulin-modified double-layered nanoparticles containing chemotherapeutics on orthotopic colon cancer. *Biomaterials*. 2022;283:121440. doi:10.1016/j.biomaterials.2022.121440
44. Lopez-Molina D, Chazarra S, How CW, et al. Cinnamate of inulin as a vehicle for delivery of colonic drugs. *Int J Pharm*. 2015;479(1):96–102. doi:10.1016/j.ijpharm.2014.12.064
45. Wirtz S, Popp V, Kindermann M, et al. Chemically induced mouse models of acute and chronic intestinal inflammation. *Nat Protocol*. 2017;12(7):1295–1309. doi:10.1038/nprot.2017.044
46. Liu ZJ, Liu F, Wang W, et al. Study of the alleviation effects of a combination of *Lactobacillus rhamnosus* and inulin on mice with colitis. *Article Food Funct*. 2020;11(5):3823–3837. doi:10.1039/c9fo02992c
47. Lee Y, Sugihara K, Gillilland MG, Jon S, Kamada N, Moon JJ. Hyaluronic acid–bilirubin nanomedicine for targeted modulation of dysregulated intestinal barrier, microbiome and immune responses in colitis. *Nature Mater*. 2019;19(1):118–126. doi:10.1038/s41563-019-0462-9

48. Wang M, Huang Q, Liu M, et al. Precisely inhibiting excessive intestinal epithelial cell apoptosis to efficiently treat inflammatory bowel disease with oral pifithrin-α embedded nanomedicine (OPEN). *Adv Mater*. 2023;35(49). doi:10.1002/adma.202309370
49. Zeng F, Wu Y, Li X, et al. Custom-made ceria nanoparticles show a neuroprotective effect by modul ating phenotypic polarization of the microglia. *Angew Chem Int Ed Engl*. 2018;57(20):5808–5812. doi:10.1002/anie.201802309
50. Baldim V, Yadav N, Bia N, et al. Polymer-coated cerium oxide nanoparticles as oxidoreductase-like catalysts. *ACS Appl Mater Interfaces*. 2020;12 (37):42056–42066. doi:10.1021/acsami.0c08778
51. Liu BW, Liu JW. Surface modification of nanozymes. *Nano Res Apr*. 2017;10(4):1125–1148. doi:10.1007/s12274-017-1426-5
52. Ma YY, Gao W, Zhang ZY, et al. Regulating the surface of nanoceria and its applications in heterogeneous catalysis. *Surface Science Reports*. 2018;73(1):36.
53. Naito Y, Takagi T, Yoshikawa T. Molecular fingerprints of neutrophil-dependent oxidative stress in inflammatory bowel disease. *Review J Gastroenterol*. 2007;42(10):787–798. doi:10.1007/s00535-007-2096-y
54. Tian T, Wang ZL, Zhang JH. Pathomechanisms of oxidative stress in inflammatory bowel disease and potential antioxidant therapies. *Oxid Med Cell Longevity*. 2017;2017(1):18.4535194. doi:10.1155/2017/4535194
55. Dudzinska E, Gryzinska M, Ognik K, Gil-Kulik P, Kocki J. Oxidative stress and effect of treatment on the oxidation product decomposition processes in IBD. *Oxid Med Cell Longevity*. 2018;7(1):7918261. doi:10.1155/2018/7918261
56. Quattrini S, Gatti S, Palpacelli A, et al. oxidative stress and antioxidant capacity biomarkers in adults and children with ibd: current update from oxibdiet trial. *Meeting Abst Gastroenterol*. 2022;162(7):S640.
57. Lee N, Choi SH, Hyeon T. Nano-sized CT contrast agents. *Adv Mater*. 2013;25(19):2641–2660. doi:10.1002/adma.201300081
58. Guo JW, Li DD, Tao H, et al. Cyclodextrin-derived intrinsically bioactive nanoparticles for treatment of acute and chronic inflammatory diseases. *Adv Mater*. 2019;31(46):1904607. doi:10.1002/adma.201904607
59. Ye B. Mesalazine preparations for the treatment of ulcerative colitis: are all created equal? *World J Gastrointest Pharmacol Therap*. 2015;6 (4):10.4292/wjgpt.v6.i4.137. doi:10.4292/wjgpt.v6.i4.137
60. Xie C, Quan RZ, Hong FJ, Zou KF, Yan W, Fu Y. The culprit of mesalamine intolerance: case series and literature review. *BMC Gastroenterol*. 2019;19138. doi:10.1186/s12876-019-1049-2
61. Bakshi HA, Mishra V, Satija S, et al. Dynamics of prolyl hydroxylases levels during disease progression in experimental colitis. *Inflammation*. 2019;42(6):2032–2036. doi:10.1007/s10753-019-01065-3
62. Chassaing B, Aitken JD, Malleshappa M, Vijay-Kumar M. Dextran sulfate sodium (DSS)-induced colitis in mice. *Curr Protocol Immunol*. 2014;104(1). [D - 9101651. (- 1934-368X (Electronic)):- 15.25.1-15.25.14]. doi:10.1002/0471142735.im1525s104
63. Wu CC, Chen JS, Wu WM, et al. Myeloperoxidase serves as a marker of oxidative stress during single haemodialysis session using two different biocompatible dialysis membranes. *Article Nephrol Dial Transplant*. 2005;20(6):1134–1139. doi:10.1093/ndt/gfh764
64. Campbell EL, Colgan SP. Control and dysregulation of redox signalling in the gastrointestinal tract. *Nat Rev Gastroenterol Hepatol*. 2019;16 (2):106–120. doi:10.1038/s41575-018-0079-5
65. Yang J, Xiao S, Deng J, et al. Oxygen vacancy-engineered cerium oxide mediated by copper-platinum exhibit enhanced SOD/CAT-mimicking activities to regulate the microenvironment for osteoarthritis therapy. *J Nanobiotechnol*. 2024;22(1):491. doi:10.1186/s12951-024-02678-z
66. Chen X, He Q, Zhai Q, et al. Adaptive nanoparticle-mediated modulation of mitochondrial homeostasis and inflammation to enhance infected bone defect healing. *ACS Nano*. 2023;17(22):22960–22978. doi:10.1021/acsnano.3c08165
67. Jeong HG, Cha BG, Kong DW, et al. Ceria nanoparticles fabricated with 6-aminohexanoic acid that overcome systemic inflammatory response syndrome. *Adv Healthcare Mater*. 2019;8(9):1801548. doi:10.1002/adhm.201801548
68. Gupta A, Das S, Neal CJ, Seal S. Controlling the surface chemistry of cerium oxide nanoparticles for biological applications. *J Mat Chem B*. 2016;4 (19):3195–3202. doi:10.1039/c6tb00396f
69. Chadha S, Kumar A, Srivastava SA, Behl T, Ranjan R. Inulin as a delivery vehicle for targeting colon-specific cancer. *Curr Drug Deliv*. 2020;17 (8):651–674. doi:10.2174/1567201817666200527133719
70. Hufnagel B, Muellner V, Hlatky K, et al. Chemically modified inulin for intestinal drug delivery - A new dual bioactivity concept for inflammatory bowel disease treatment. *Carbohydr Polym*. 2021;252:9.117091. doi:10.1016/j.carbpol.2020.117091
71. Gruskiene R, Lavelli V, Sereikaite J. Application of inulin for the formulation and delivery of bioactive molecules and live cells. *Article Carbohydr Polym*. 2024;327:15.121670. doi:10.1016/j.carbpol.2023.121670
72. Karagozian R, Burakoff R. The role of mesalamine in the treatment of ulcerative colitis. 1176-6336 (Print).
73. Han RZ, He HS, Lu Y, Lu HP, Shen S, Wu W. Oral targeted drug delivery to post-gastrointestinal sites. *J Control Release*. 2024;370:256–276. doi:10.1016/j.jconrel.2024.04.047
74. Afinjuomo F, Abdella S, Youssef SH, Song YM, Garg S. Inulin and its application in drug delivery. *Pharmaceuticals*. 2021;14(9):855. doi:10.3390/ph14090855